

Are your **MRI contrast agents** cost-effective?

Learn more about generic **Gadolinium-Based Contrast Agents**.



**FRESENIUS
KABI**

caring for life

AJNR

Cerebral White Matter Disruption in Creutzfeldt-Jakob Disease

H. Lee, O.S. Cohen, H. Rosenmann, C. Hoffmann, P.B. Kingsley, A.D. Korczyn, J. Chapman and I. Prohovnik

AJNR Am J Neuroradiol published online 10 May 2012
<http://www.ajnr.org/content/early/2012/05/10/ajnr.A3125>

This information is current as
of April 20, 2024.

ORIGINAL
RESEARCH

H. Lee
O.S. Cohen
H. Rosenmann
C. Hoffmann
P.B. Kingsley
A.D. Korczyn
J. Chapman
I. Prohovnik



Cerebral White Matter Disruption in Creutzfeldt-Jakob Disease

BACKGROUND AND PURPOSE: Human prion diseases are known to cause gray matter degeneration in specific cerebral structures, but evidence for white matter involvement is scarce. We used DTI to test the hypothesis that white matter integrity is disrupted in human CJD during the early stages of the disease.

MATERIALS AND METHODS: Twenty-one patients with the E200K variant of CJD and 19 controls participated in DTI studies conducted on a 1.5T MR imaging scanner. The data were quantitatively analyzed and mapped with a voxelwise TBSS method.

RESULTS: We found significant reductions of FA in patients with CJD in distinct and functionally relevant white matter pathways, including the corticospinal tract, internal capsule, external capsule, fornix, and posterior thalamic radiation. Moreover, these FA deficits increased with disease duration, and were mainly determined by increase of radial diffusivity, suggesting elevated permeability of axonal membranes.

CONCLUSIONS: The findings suggest that some of the symptoms of CJD may be caused by a functional disconnection syndrome, and that the leukoencephalopathy is progressive and detectable fairly early in the course of the disease.

ABBREVIATIONS: AD = axial diffusivity; CJD = Creutzfeldt-Jakob disease; FA = fractional anisotropy; MD = mean diffusivity; MMSE = Mini-Mental State Examination; RD = radial diffusivity; TBSS = tract-based spatial statistics

Human prion diseases present a scientific challenge and a public health concern. The putative pathogenic agent is unlike any other: it lacks nucleic acids and conventional genetic material, it demonstrates extraordinary resistance to chemical and physical inactivation, and its reproduction and infectivity may be mediated primarily by conformational changes.¹ CJD is the most common human prion disease, and its etiology can be inherited, infectious, or sporadic. Clinical presentation is characterized by rapidly progressive dementia, ataxia, and myoclonus, and it is invariably fatal; typical duration of survival after onset ranges from a few months to a year.

The early evolution of CJD in the human brain is not well understood. Neuropathologic studies demonstrate deposition of the abnormal prion protein (PrP^{Sc}), astrogliosis, spongiform change, and neuronal loss in the striatum, thalamus, cerebellum, and cortex,² but these observations are typically made at terminal disease stages. Recent neuroimaging work

with DWI has confirmed the involvement of these structures at early stages of the disease,³⁻⁶ but these studies were all focused on reduced diffusion in cerebral gray matter, thought to reflect the PrP^{Sc} deposition and/or vacuolation.^{7,8} It is likely that PrP^{Sc} propagates along white matter pathways,^{9,10} and such propagation studies may reveal the spread of the pathogen in the human brain. We aimed to test the hypothesis that there is a specific white matter dysfunction in the early stages of CJD. We assessed WM integrity by DTI, a method of quantifying displacement of water molecules that are interacting with surrounding microstructural environments, such as cell membranes, macromolecules, and nerve fibers.

Materials and Methods

Subjects

As part of a prospective imaging study of CJD, 21 patients with familial CJD and 19 healthy controls from the same families were recruited. Patients all had a clinical diagnosis of probable CJD by World Health Organization criteria,¹¹ with at least 2 of the following: rapidly progressive dementia, myoclonus, visual or cerebellar symptoms, pyramidal or extrapyramidal dysfunction, or akinetic mutism. To ensure correct diagnosis, all patients were confirmed positive for the E200K mutation of the *PRNP* gene and all were followed until death. MR imaging scans were conducted early in the course of the disease, an average of 2.81 ± 2.02 months from symptomatic onset, when they were, generally, not yet demented. The controls were members of the same families who were confirmed to be negative to the E200K mutation, healthy by history, and had medical and neurologic examinations and neuropsychological testing. The study was approved by the institutional review boards of the Sheba Medical Center, Israel, and the Mount Sinai School of Medicine, New York.

Received January 16, 2012; accepted after revision February 21.

From the Departments of Psychiatry (H.L., I.P.) and Radiology (I.P.), Mount Sinai School of Medicine, New York, New York; Department of Neurology (H.R.), Hadassah University Hospital, Jerusalem, Israel; Departments of Neurology (O.S.C., J.C.) and Radiology (C.H.), Sheba Medical Center, and Sieratzky Chair of Neurology, Sackler Faculty of Medicine (A.D.K.), Tel Aviv University, Tel Aviv, Israel; Sackler Faculty of Medicine (O.S.C., J.C.), Tel Aviv University, Tel Aviv, Israel; and Department of Radiology (P.B.K.), North Shore University Hospital, Manhasset, New York.

This study was supported by NIH grant # NS043488 (Dr. Isak Prohovnik).

A preliminary account of this work was presented at International Society for Magnetic Resonance in Medicine, May 1-7, 2010, Stockholm, Sweden.

Please address correspondence to Dr. Isak Prohovnik, Department of Psychiatry, Box 1230, One Gustave Levy Place, New York, NY 10029; e-mail: Isak.Prohovnik@mssm.edu



Indicates open access to non-subscribers at www.ajnr.org

<http://dx.doi.org/10.3174/ajnr.A3125>

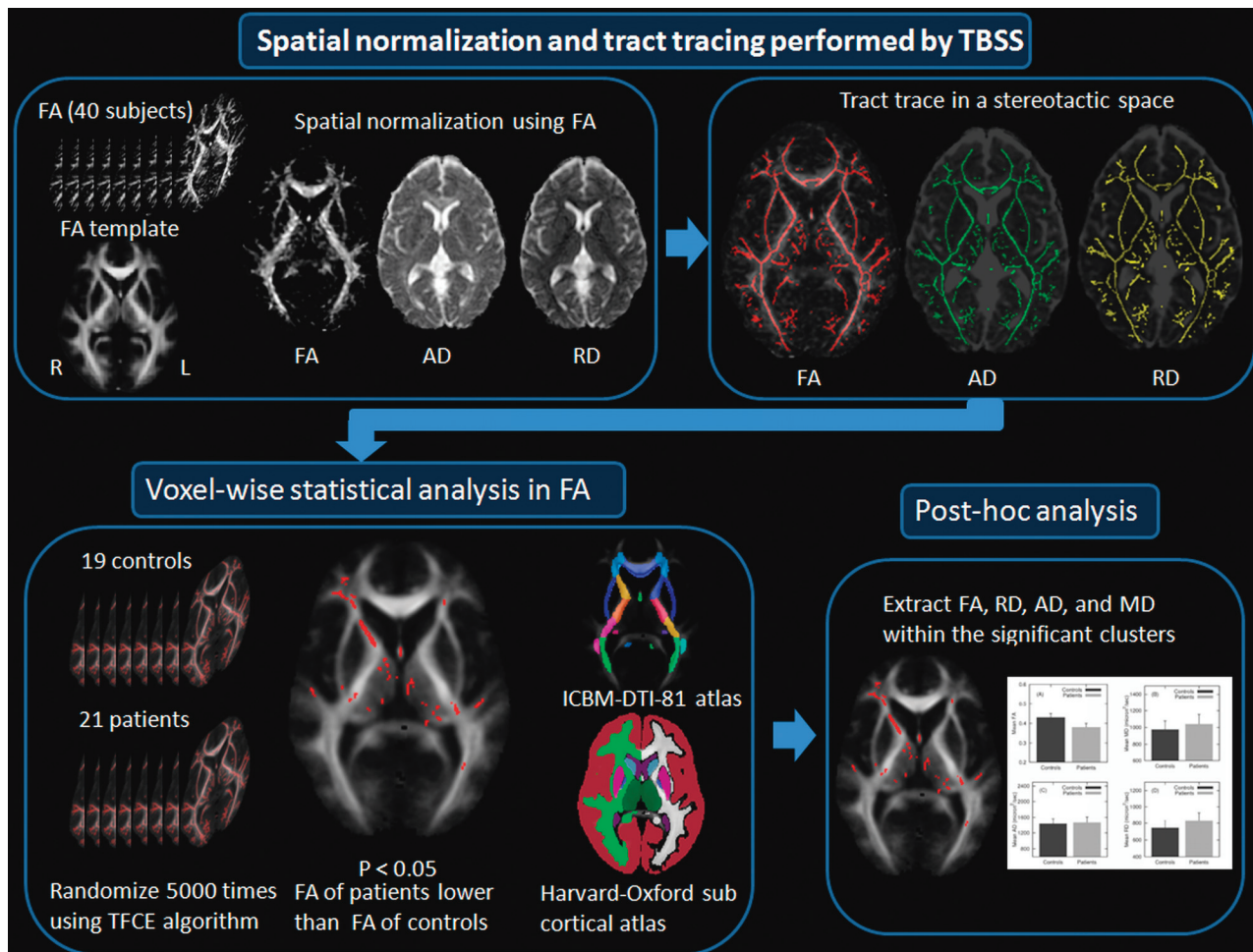


Fig 1. A flow diagram of voxelwise analysis performed by TBSS. After spatial normalization to a stereotactic space using a default FMRIB58_FA template, tracts are traced in FA, AD, and RD maps. Voxels surviving $P < .05$ (corrected for multiple comparisons) are overlaid onto a group averaged FA map and their anatomic correspondence is defined by ICBM-DTI-81 white matter and Harvard-Oxford subcortical structural atlases.

MR Imaging Acquisition

Scanning was performed at the Sheba Medical Center, Israel, on a 1.5T Signa Excite system (GE Healthcare, Milwaukee, Wisconsin) with a standard quadrature head coil. As part of the standardized study protocol, MR imaging sequences included a single-shot echo-planar pulsed gradient spin-echo DTI sequence, with $b = 1000$ seconds/mm². Imaging parameters include 25 contiguous 5-mm axial sections, FOV 260 mm, TR 8300 ms, TE 94 ms, flip angle 90°, with an acquisition matrix of 128×128 , zero-filled to 256×256 , yielding the reconstructed in-plane image resolution of 1.0×1.0 mm. The DTI sequence acquired a non-diffusion-weighted image ($b = 0$ seconds/mm², T2-weighted) and a diffusion-weighted image ($b = 1000$ seconds/mm²) along each of 25 noncollinear gradient directions.

Occasionally, severe signal loss in a diffusion-weighted image was detected, and inclusion of the artifacts led to erroneously derived DTI indices. For quality assurance purposes, we discarded a DTI volume if the mean intensity of a section was more than 4 standard deviations below the mean of all 25 DWI volumes. Of the 1040 volumes in the study, a total of 29 volumes (5 in controls and 24 in patients) were discarded. The artifact was not spatially selective, and it is not clear whether it was related to a scanner malfunction, bulk head movement, or CSF pulsation.¹²

Image Analysis

Voxelwise image processing was performed by the FDT (diffusion toolbox) and TBSS tools provided by FMRIB software (<http://www.fmrib.ox.ac.uk/fsl/>).¹³ For each subject, motion and eddy current distortion were reduced by registering each diffusion-weighted image with its $b = 0$ image with affine transformation using FLIRT.¹⁴ A binary brain mask was created by applying the BET¹⁵ tool to the $b = 0$ image. The 6 tensor elements were calculated by a linear least-square fitting method, and 3 eigenvalues ($\lambda_1 > \lambda_2 > \lambda_3$) were derived.

We evaluated 4 common indices: MD, RD (diffusivity perpendicular to the principal axis, ie, across the axonal membrane), AD (diffusivity along the principal axis, ie, within the axonal length), and FA.

DTI Voxelwise Analysis

Final analysis was performed by TBSS.¹⁶ In the spatial normalization step, individual FA maps were warped to match the default FMRIB58_FA template, using a nonlinear registration algorithm (FNIRT), to fit the standard Montreal Neurological Institute stereotactic space. Residual misregistration was reduced by tracing tract centers within thick fiber bundles, transforming 3D fiber bundles into a “skeleton,” thereby ensuring exclusion of other tissue or fluid.¹⁶ Last, both nonlinear transformation and projection parameters derived from the FA maps were applied onto corresponding MD, RD,

Table 1. Patient characteristics (mean \pm SD of numeric variables)

Total number	21
Age (years)	59.4 \pm 7.4
Male/Female	13/8
MMSE	20.9 \pm 6.7
Clinical Neurological Scale	12.1 \pm 5.8
Duration of illness (months)	2.8 \pm 2.0
Survival after MRI (months)	4.3 \pm 4.7
Symptoms (%)	
Brain stem dysfunction	57%
Frontal release signs	86
Cerebellar signs	90
Extrapyramidal signs	86
Pyramidal signs	76
Cognitive impairment (MMSE<24)	60

and AD images to produce skeletonized maps of the 4 DTI indices, as shown in Fig 1.

Voxelwise statistical analysis was performed on thresholded (0.2) skeletonized FA maps by the nonparametric randomization method with age entered as a covariate. Significance was determined by the threshold-free cluster extent algorithm¹⁷ at $P < .05$, corrected for a multiple comparison. To maintain a conservative approach, all significance tests were 2-tailed. The cerebellum was only partially ana-

lyzed, due to incomplete brain coverage of some subjects. Anatomic locations of significant clusters were determined by the ICBM-DTI-81 WM labels atlas^{18,19} for the internal capsule, external capsule, corpus callosum, and cerebral peduncles; by the Harvard-Oxford subcortical structural atlases (<http://www.cma.mgh.harvard.edu/>) for the brain stem and thalamus; and by the Talairach atlas (<http://ric.uthscsa.edu/>) for the frontal lobe. FA, MD, AD, and RD values were also extracted from the skeletonized regions where FA differences were significant. The extracted values were then subjected to post hoc regression analyses.

Results

Controls ($n = 19$, age 56.6 \pm 9.9 years, 9 men) were free of cognitive deficits, as measured by the MMSE²⁰ (28.8 \pm 1.5), and neurologic symptoms, as measured by the structured Clinical Neurological Scale³ (0.5 \pm 0.8). Patients did not differ from controls on age or sex distribution and demonstrated the expected symptoms (Table 1); they survived 4.25 \pm 4.73 months after the MR imaging scans.

No voxels demonstrated higher FA in patients than controls. Voxelwise analysis of the white matter revealed decreased FA among the patients in the brain stem, cerebral pe-

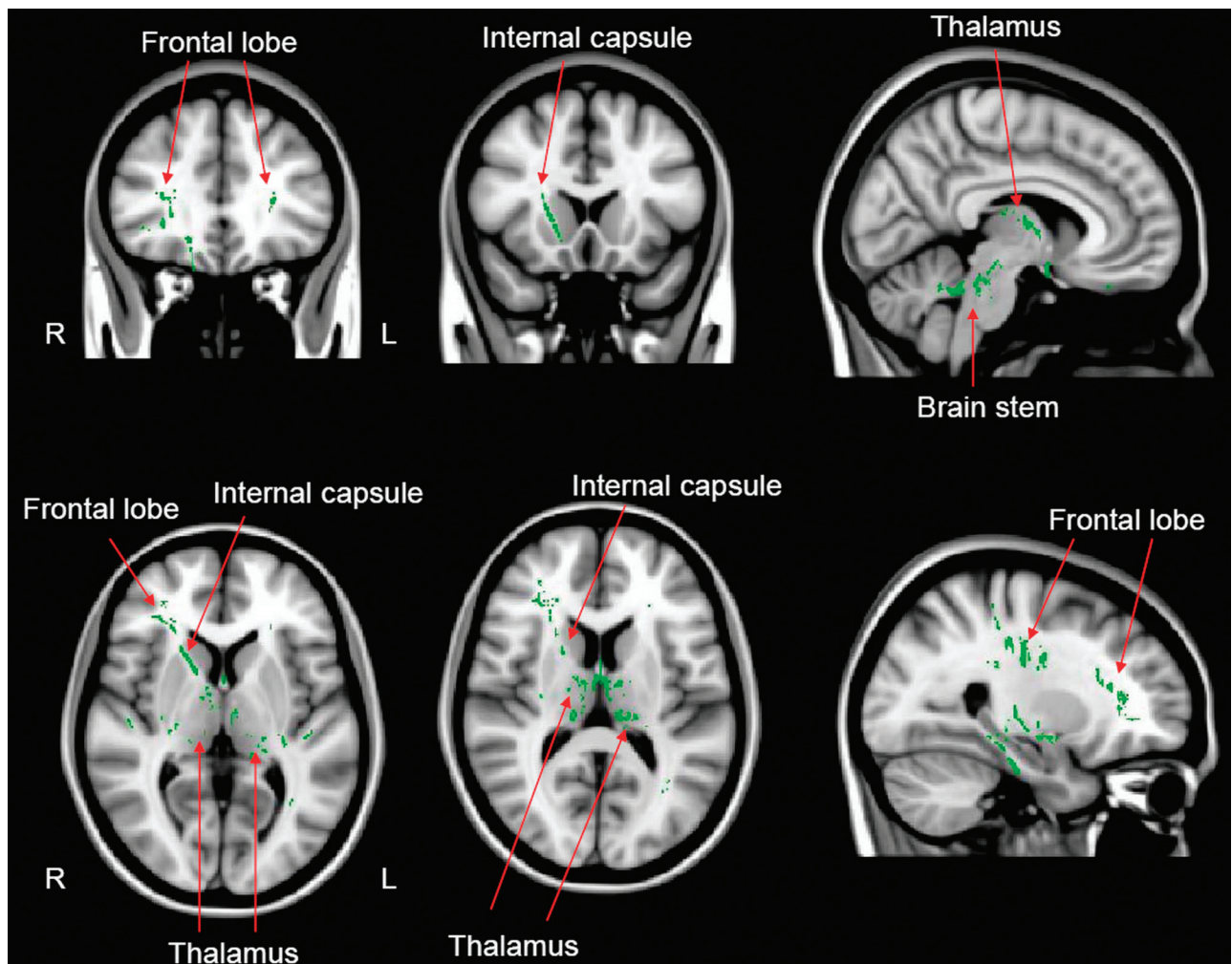


Fig 2. Pattern of reduced fractional anisotropy (green) in patients with CJD compared with healthy normal controls. Results are overlaid onto a representative anatomic scan in Montreal Neurological Institute standard brain (MNI152) stereotactic space. Arrows indicate corresponding anatomic regions. Voxels are considered significant at a threshold of $P < .05$ (corrected for multiple comparisons).

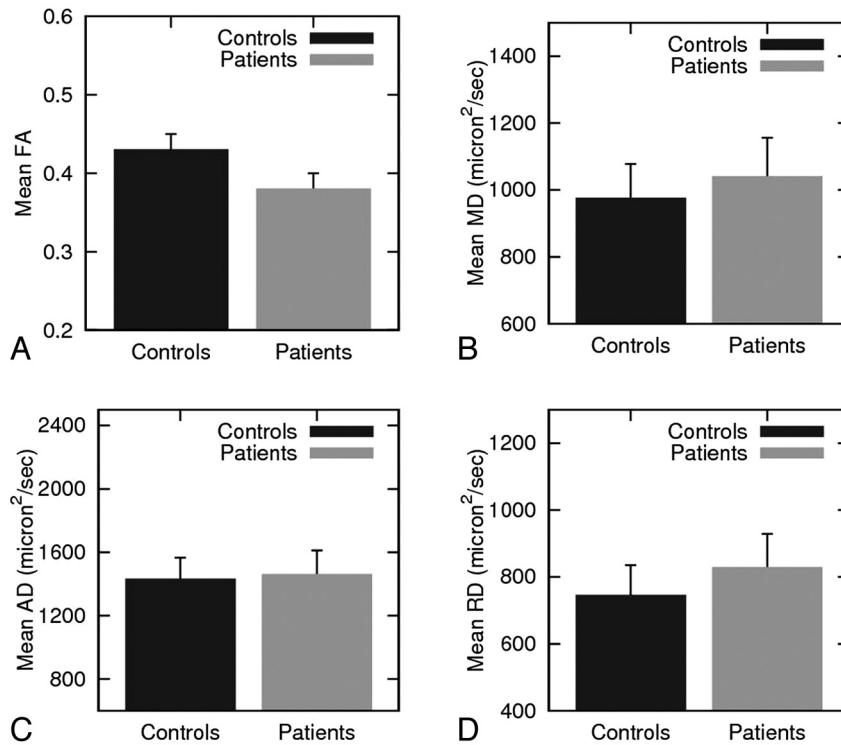


Fig 3. Group averaged DTI indices of the significant voxels shown in Fig 1. Group averaged values of (A) FA, (B) MD, (C) AD, and (D) RD are plotted by diagnosis. The error bars represent standard deviations.

duncle, cerebellar peduncle, corticospinal tract, thalamus, internal capsule (anterior limb, posterior limb, and retrolenticular), external capsule, fornix, corpus callosum, and frontal lobe, including corona radiata (anterior, superior, and posterior), posterior thalamic radiation, and sagittal striatum. The color-coded voxels in Fig 2 represent significantly reduced FA in patients. Within those clusters, group average MD, AD, and RD were derived as shown in Fig 3, and corresponding percentage group differences were calculated. Mean FA values were 0.43 ± 0.02 in controls and 0.38 ± 0.02 in patients ($t_{37} = 6.61, P < .0001$). On average, FA in patients was 12% lower than in controls, and MD was elevated by 7%. Comparison of axial and radial diffusivities within the same clusters indicated nearly equal axial diffusivities between the groups (within 2%), while radial diffusivity was substantially elevated (11%) among the patients. The mean FA of the significant voxels was significantly correlated with duration of illness within the patients ($r = -0.51, P < .02$; Fig 4). The linear regression equation ($FA = 0.397 - 0.0055 \times \text{Duration}$) indicates that the FA deficit, compared with controls, would increase from approximately 8% at duration 0 (onset of disease) to approximately 20% after 10 months.

Discussion

Gray matter neuropathology at the terminal stage of disease is well described in CJD and primarily involves the cerebellum, striatum, thalamus, and cortex. There is also emerging consensus regarding imaging findings at early stages of the disease, which consist of reduced diffusion of striatum and thalamus. DWI is not sensitive to cerebellar degeneration,³ and cortical diffusion reductions are easily detectable only in individual patients; it is not yet established why these are elusive in group

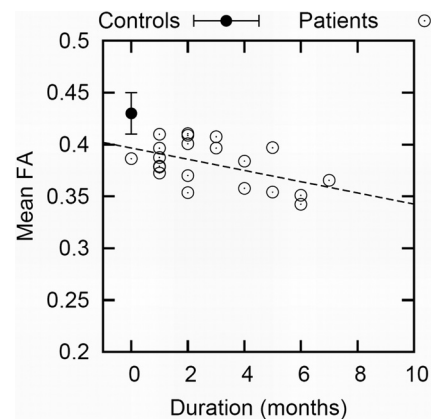


Fig 4. Pearson product-moment correlation between duration of illness and averaged FA over the significant voxels. Open circles represent mean FA values of each patient. The filled circles and error bar represent the mean and standard deviations of FA in controls.

analyses.⁵ All these brain areas are richly interconnected by known white matter pathways, and constitute known functional circuits concerned primarily with movement control. Prions are suspected to propagate along axonal tracts, and the extensive connectivity among the known gray matter sites of degeneration in CJD should reveal this propagation.

In animal models of prion infection, it is clear that prions can invade the brain through peripheral neuronal pathways.^{9,21,22} Animal models of CJD also demonstrate white matter deposition of PrP^{Sc}, astrocytes, and vacuolization, all of which are hallmarks of CJD pathology, as well as damage to myelinated axons.^{1,10,23-26} Recently, new evidence is accumulating to suggest a fundamental relationship of the prion protein to WM. While predominantly neuronal, PrP^C (the nor-

mal cellular precursor protein) is also expressed in astrocytes and oligodendrocytes.²⁷ PrP^C appears to be necessary for myelin protection and maintenance²⁸; its replacement by PrP^{Sc} in CJD may well cause myelinopathy. This finding has now been extended to the early development of Prnp 0/0 mice, which display deficits in motor coordination and balance and vacuolation in several WM tracts at age 6 months.²⁹

In the human brain, pathologic studies of terminal CJD reported axonal damage, and suggested the possibility of retrograde axonal transport of prions, infecting multiple sites along neuroanatomic pathways.^{27,30-32} In the Japanese panencephalopathic variant (pCJD), WM damage has been noted in the internal capsule, brain stem, and middle cerebellar peduncles,³³ consistent with our imaging findings. In vCJD (the variant CJD associated with consumption of tainted beef), vacuolation, PrP deposition, and glial cell reaction were observed in the cortical WM of all 11 cases studied.³⁴ The suggestion was made that PrP^{Sc} was leaking from damaged axons, and the cerebral cortex may be affected by prion pathology spreading through ascending fiber tracts. However, human WM findings are scarce in sporadic CJD, the most common sporadic type.³⁵⁻³⁷

It is plausible, thus, that white matter pathways between the injured gray matter sites are affected in CJD, but robust evidence has been lacking until now. The current study provides such evidence through DTI-derived indices: FA, MD, RD, and AD. FA is the most widely reported quantitative index in DTI and is known to reflect white matter integrity.³⁸ High FA appears in densely packed WM tracts where displacement of water molecules perpendicular to the fibers (radial diffusivity) is restricted by the barriers of myelinated axons, but water movement is less restricted in the direction parallel to the axonal fibers (axial diffusivity). MD is an average of the 3 diffusion coefficients, highly sensitive to CJD in gray matter.^{5,7,39} In the current whole-brain voxelwise quantitative analysis, we found significant reduction of FA in corticospinal tracts, basal ganglia pathways, thalamus, and cerebellar peduncles. Moreover, these FA reductions were progressive and became worse with longer disease duration. The pathways that were found to be significantly affected in the current study are well known to mediate the connectivity among the thalamus, striatum, and frontal cortex. Notably, the cerebellar peduncles, which play a central role in connecting the cerebellum with brain stem and thalamus, were also affected. Previously, we reported significant cerebellar atrophy around the fourth ventricle in patients with CJD with definite cerebellar symptoms, and suggested that the atrophy may mask diffusion reductions.³ Considering our current findings, it is also reasonable to consider cerebellar symptoms as a result of disrupted efferent fibers emanating from the cerebellum to other structures.

The precise biophysical basis of the FA reductions observed here, and thus the cellular pathology, is unknown. Identifying the tissue substrate of FA changes is complicated by the fact that diffusion of water molecules occurs in at least 2 compartments: intracellular and extracellular. FA was shown to be elevated with increasing myelination,⁴⁰⁻⁴² and it is tempting to interpret our data as proof of degraded myelination. However, the axonal environment can be altered by other mechanisms that would modify diffusion, such as geometry. It is noteworthy, however, that our data strongly suggest that FA reductions

are mostly determined by an increase in RD. This component of diffusivity is thought to reflect water molecules experiencing the barriers of surrounding myelinated axons.⁴³ The data are thus consistent with the notion that fibers are less insulated from extracellular space and more permeable to water molecules. This conclusion is strongly supported by a neuropathologic study³³ that reported severe loss of myelin in panencephalopathic CJD. However, our current data cannot resolve whether the white matter changes are primary or secondary to gray matter degeneration. Prion deposition has been shown in olfactory sensory pathway of patients with sporadic CJD,⁴⁴ but it is not yet established whether this is caused by centrifugal or centripetal propagation.^{33,45} While the regression against duration of disease suggests that white matter integrity is impaired before clinical onset, gray matter diffusion changes are also detectable before onset.⁵ Therefore, it is plausible that prion-associated degeneration starts in the basal ganglia and thalamus, and then spreads through ascending white matter tracts to cortical projection areas. This hypothesis can be tested by serial examinations of FA and MD in gray and white matter in the future. If confirmed, it would suggest that increasing symptoms at later stages of CJD could be a consequence of a progressive disconnection syndrome, not just further degeneration of gray matter.

Finally, we should note that this study was conducted in a homogeneous sample of familial patients with CJD with the E200K mutation. Such patients represent a minority (less than 20%) of the affected population, which is mostly composed of sporadic patients. The neuropathologic features of E200K patients and their DWI signature are similar to sporadic patients,⁵ but there are no data comparing them in white matter properties. It is possible, though unlikely, that the current findings of progressive focal leukoencephalopathy in distinct pathways is unique to the E200K variant; future work should address this in patients with sporadic CJD.

Acknowledgments

We thank Ilana Seror, MSc, Janet Ben-Mordechai, RN, and Vered Luufman-Malkin, BA, for their assistance in the study. Most importantly, we are indebted to the patients, healthy subjects, and their families, without whose help this work could not have been accomplished. H.L. and O.S.C. contributed equally to this work.

References

1. Prusiner SB. Prions. *Proc Natl Acad Sci USA* 1998;95:13363-83
2. Masters CL, Richardson EP Jr. Subacute spongiform encephalopathy (Creutzfeldt-Jakob disease). The nature and progression of spongiform change. *Brain* 1978;101:333-44
3. Cohen OS, Hoffmann C, Lee H, et al. MRI detection of the cerebellar syndrome in Creutzfeldt-Jakob disease. *Cerebellum* 2009;8:373-81
4. Kallenberg K, Schulz-Schaeffer WJ, Jastrow U, et al. Creutzfeldt-Jakob disease: comparative analysis of MR imaging sequences. *AJNR Am J Neuroradiol* 2006;27:1459-62
5. Lee H, Rosenmann H, Chapman J, et al. Thalamo-striatal diffusion reductions precede disease onset in prion mutation carriers. *Brain* 2009;132:2680-87
6. Young GS, Geschwind MD, Fischbein NJ, et al. Diffusion-weighted and fluid-attenuated inversion recovery imaging in Creutzfeldt-Jakob disease: high sensitivity and specificity for diagnosis. *AJNR Am J Neuroradiol* 2005;26:1551-62
7. Manners DN, Parchi P, Tonon C, et al. Pathologic correlates of diffusion MRI changes in Creutzfeldt-Jakob disease. *Neurology* 2009;72:1425-31
8. Geschwind MD, Potter CA, Sattavat M, et al. Correlating DWI MRI with patho-

- logic and other features of Jakob-Creutzfeldt disease. *Alzheimer Dis Assoc Disord* 2009;23:82–87
9. Fraser H, Dickinson AG. Targeting of scrapie lesions and spread of agent via the retino-tectal projection. *Brain Res* 1985;346:32–41
 10. Taraboulos A, Jendroska K, Serban D, et al. Regional mapping of prion proteins in brain. *Proc Natl Acad Sci U S A* 1992;89:7620–24
 11. World Health Organization. Global surveillance, diagnosis and therapy of human transmissible spongiform encephalopathies: report of a WHO consultation. In: *Emerging and Other Communicable Diseases, Surveillance and Control*. Geneva, Switzerland: World Health Organization; 1998
 12. Skare S, Andersson JL. On the effects of gating in diffusion imaging of the brain using single shot EPI. *Magn Reson Imaging* 2001;19:1125–28
 13. Smith SM, Jenkinson M, Woolrich MW, et al. Advances in functional and structural MR image analysis and implementation as FSL. *Neuroimage* 2004;23:S208–19
 14. Jenkinson M, Smith S. A global optimisation method for robust affine registration of brain images. *Med Image Anal* 2001;5:143–56
 15. Smith SM. Fast robust automated brain extraction. *Hum Brain Mapp* 2002;17:143–55
 16. Smith SM, Jenkinson M, Johansen-Berg H, et al. Tract-based spatial statistics: voxelwise analysis of multi-subject diffusion data. *Neuroimage* 2006;31:1487–505
 17. Smith SM, Nichols TE. Threshold-free cluster enhancement: addressing problems of smoothing, threshold dependence and localisation in cluster inference. *Neuroimage* 2009;44:83–98
 18. Wakana S, Caprihan A, Panzenboeck MM, et al. Reproducibility of quantitative tractography methods applied to cerebral white matter. *Neuroimage* 2007;36:630–44
 19. Mori S, Crain BJ. *MRI Atlas of Human White Matter*. Amsterdam, the Netherlands: Elsevier; 2005
 20. Folstein MF, Folstein SE, McHugh PR. “Mini-mental state.” A practical method for grading the cognitive state of patients for the clinician. *J Psychiatr Res* 1975;12:189–98
 21. Kimberlin RH, Walker CA. Pathogenesis of mouse scrapie: dynamics of agent replication in spleen, spinal cord and brain after infection by different routes. *J Comp Pathol* 1979;89:551–62
 22. Kimberlin RH, Field HJ, Walker CA. Pathogenesis of mouse scrapie: evidence for spread of infection from central to peripheral nervous system. *J Gen Virol* 1983;64:713–16
 23. Bouzamondo-Bernstein E, Hopkins SD, Spilman P, et al. The neurodegeneration sequence in prion diseases: evidence from functional, morphological and ultrastructural studies of the GABAergic system. *J Neuropathol Exp Neurol* 2004;63:882–99
 24. Brandner S, Isenmann S, Raeber A, et al. Normal host prion protein necessary for scrapie-induced neurotoxicity. *Nature* 1996;379:339–43
 25. Jendroska K, Heinzl FP, Torchia M, et al. Proteinase-resistant prion protein accumulation in Syrian hamster brain correlates with regional pathology and scrapie infectivity. *Neurology* 1991;41:1482–90
 26. Safar JG, Geschwind MD, Deering C, et al. Diagnosis of human prion disease. *Proc Natl Acad Sci USA* 2005;102:3501–06
 27. Prinz M, Montrasio F, Furukawa H, et al. Intrinsic resistance of oligodendrocytes to prion infection. *J Neurosci* 2004;24:5974–81
 28. Radovanovic I, Braun N, Giger OT, et al. Truncated prion protein and Doppel are myelinotoxic in the absence of oligodendrocytic PrP^C. *J Neurosci* 2005;25:4879–88
 29. Nazor KE, Seward T, Telling GC. Motor behavioral and neuropathological deficits in mice deficient for normal prion protein expression. *Biochim Biophys Acta* 2007;1772:645–53
 30. Liberski PP, Yanagihara R, Gibbs CJ, et al. White matter ultrastructural pathology of experimental Creutzfeldt-Jakob disease in mice. *Acta Neuropathol* 1989;79:1–9
 31. Liberski PP, Yanagihara R, Gibbs CJ, et al. Spread of Creutzfeldt-Jakob disease virus along visual pathways after intraocular inoculation. *Arch Virol* 1990;111:141–47
 32. Liberski PP, Budka H. Neuroaxonal pathology in Creutzfeldt-Jakob disease. *Acta Neuropathol* 1999;97:329–34
 33. Matsusue E, Kinoshita T, Sugihara S, et al. White matter lesions in panencephalopathic type of Creutzfeldt-Jakob disease: MR imaging and pathologic correlations. *AJNR Am J Neuroradiol* 2004;25:910–18
 34. Armstrong RA. A quantitative study of the pathological changes in the cortical white matter in variant Creutzfeldt-Jakob disease (vCJD). *Clin Neuropathol* 2010;29:390–96
 35. Bell JE, Ironside JW. Neuropathology of spongiform encephalopathies in humans. *Br Med Bull* 1993;49:738–77
 36. Fraser E, McDonagh AM, Head M, et al. Neuronal and astrocytic responses involving the serotonergic system in human spongiform encephalopathies. *Neuropathol Appl Neurobiol* 2003;29:482–95
 37. Cali I, Castellani R, Yuan J, et al. Classification of sporadic Creutzfeldt-Jakob disease revisited. *Brain* 2006;129:2266–77
 38. Beaulieu C. The basis of anisotropic water diffusion in the nervous system—a technical review. *NMR Biomed* 2002;15:435–55
 39. Fulbright RK, Hoffmann C, Lee H, et al. MR imaging of familial Creutzfeldt-Jakob disease: a blinded and controlled study. *AJNR Am J Neuroradiol* 2008;29:1638–43
 40. Baratti C, Barnett AS, Pierpaoli C. Comparative MR imaging study of brain maturation in kittens with T1, T2, and the trace of the diffusion tensor. *Radiology* 1999;210:133–42
 41. Li TQ, Chen ZG, Hindmarsh T. Diffusion-weighted MR imaging of acute cerebral ischemia. *Acta Radiol* 1998;39:460–73
 42. Neil JJ, Shiran SI, McKinstry RC, et al. Normal brain in human newborns: apparent diffusion coefficient and diffusion anisotropy measured by using diffusion tensor MR imaging. *Radiology* 1998;209:57–66
 43. Seal ML, Yucel M, Fornito A, et al. Abnormal white matter microstructure in schizophrenia: a voxelwise analysis of axial and radial diffusivity. *Schizophr Res* 2008;101:106–10
 44. Zanusso G, Ferrari S, Benedetti D, et al. Different prion conformers target the olfactory pathway in sporadic Creutzfeldt-Jakob disease. *Ann N Y Acad Sci* 2009;1170:637–43
 45. Kucharczyk W, Bergeron C. Primary white matter involvement in sporadic type Creutzfeldt-Jakob disease? Which came first, the chicken or the egg? *AJNR Am J Neuroradiol* 2004;25:905–06